

RESEARCH

Open Access



Untargeted metabolomics reveals homogeneity and heterogeneity between physiological and pathological ovarian aging

Lihua Zeng^{1,2,3,4†}, Yunyi Liang^{1,2,3†}, Lizhi Huang^{1,2,3}, Zu'ang Li^{1,2,3}, Manish Kumar⁴, Xiasheng Zheng³, Jing Li^{1,2,3}, Songping Luo^{1,2,3} and Ling Zhu^{1,2,3*} 

Abstract

Background Ovarian aging is the main cause of reduced reproductive life span, yet its metabolic profiles remain poorly understood. This study aimed to reveal the metabolic homogeneity and heterogeneity between physiological and pathological ovarian aging.

Methods Seventy serum samples from physiological ovarian aging participants, pathological ovarian aging participants (including diminished ovarian reserve (DOR), subclinical premature ovarian insufficiency (scPOI) and premature ovarian insufficiency (POI)), as well as healthy participants were collected and analyzed by untargeted metabolomics.

Results Five homogeneous differential metabolites (neopterin, menaquinone, sphingomyelin (SM) (d14:1/24:2), SM (d14:0/21:1) and SM (d17:0/25:1)) were found in both physiological and pathological ovarian aging. While five distinct metabolites, including phosphoglyceride (PC) (17:0/18:2), PC (18:2e/17:2), SM (d22:1/14:1), SM (d14:1/20:1) and 4-hydroxyretinoic acid were specific to pathological ovarian aging. Functional annotation of differential metabolites suggested that folate biosynthesis, ubiquinone and other terpenoid-quinone biosynthesis pathways, were mainly involved in the ovarian aging process. Meanwhile, dopaminergic synapses pathway was strongly associated with scPOI, vitamin digestion and absorption and retinol metabolism were associated with POI. Furthermore, testosterone sulfate, SM (d14:0/28:1), PC (18:0e/4:0) and 4-hydroxyretinoic acid, were identified as potential biomarkers for diagnosing physiological ovarian aging, DOR, scPOI, and POI, respectively. Additionally, SM (d14:1/24:2) strongly correlated with both physiological and pathological ovarian aging. 4-hydroxyretinoic acid was strongly correlated with pathological ovarian aging.

Conclusions Metabolic homogeneity of physiological and pathological ovarian aging was related to disorders of lipid, folate, ubiquinone metabolism, while metabolic heterogeneity between them was related to disorders of lipid, vitamin and retinol metabolism.

Clinical trial number Not applicable.

[†]Lihua Zeng and Yunyi Liang have contributed equally to this work.

*Correspondence:

Ling Zhu
zhulinggyn@hotmail.com; zhuling1656@gzucm.edu.cn

Full list of author information is available at the end of the article



© The Author(s) 2025. **Open Access** This article is licensed under a Creative Commons Attribution-NonCommercial-NoDerivatives 4.0 International License, which permits any non-commercial use, sharing, distribution and reproduction in any medium or format, as long as you give appropriate credit to the original author(s) and the source, provide a link to the Creative Commons licence, and indicate if you modified the licensed material. You do not have permission under this licence to share adapted material derived from this article or parts of it. The images or other third party material in this article are included in the article's Creative Commons licence, unless indicated otherwise in a credit line to the material. If material is not included in the article's Creative Commons licence and your intended use is not permitted by statutory regulation or exceeds the permitted use, you will need to obtain permission directly from the copyright holder. To view a copy of this licence, visit <http://creativecommons.org/licenses/by-nc-nd/4.0/>.

Keywords Untargeted metabolomics, Serum metabolic biomarkers, Lipids, Physiological ovarian aging, Pathological ovarian aging

Introduction

Reproductive decline is the earliest onset symptom of aging in females [1, 2]. The ovaries, which produce oocytes and steroid hormones, are essential reproductive organs for female reproductive development, fertility maintenance, and endocrine homeostasis [3, 4].

Ovarian aging leads to infertility and menopause due to reduced oocyte quality and quantity, and decreased ovarian function. Physiological ovarian aging gradually occurs with advancing development with age, with 35 years being commonly regarded as the onset of this process [5, 6]. In contrast, pathological ovarian aging can arise from various causes, including hereditary, immune, medical, endocrine, inflammatory, lifestyle, and socio-psychological factors [7–9].

Pathological ovarian aging is a progressive condition that is subdivided into several stages: diminished ovarian reserve (DOR), poor ovarian response (POR), subclinical premature ovarian insufficiency (scPOI) and premature ovarian insufficiency (POI). The incidence of pathological ovarian aging is rising and it often occurs earlier in life. Among infertile women, 29.3 – 30% are diagnosed with DOR [10, 11], with up to one-third of these patients also experienced POR [12]. Notably, DOR can progress to POI within months to several years. The prevalence of POI is 1.8 – 3.7%, and 0.4% of cases occurring in women younger than 35 years old [13, 14].

Although physiological and pathological ovarian aging share similar clinical symptoms, including hormonal changes and eventual ovarian failure, the extent to which these two types of ovarian aging are similar, as well as the underlying mechanisms driving their differences and progression, remain largely unknown. A better understanding of these similarities and differences could enhance early detection of ovarian aging, even in its early or sub-clinical stages, and provide critical insights for developing effective disease prevention and treatment strategies.

Metabolomics, a promising approach in systems biology, enables the comprehensive characterization of circulating metabolites. As metabolic changes can reflect biological physiology and pathology, metabolomics hold great potential for discovering clinical biomarkers, monitoring disease progression and evaluating therapeutic outcomes [15, 16]. Women with ovarian aging are prone to metabolic disorders, particularly those involving lipid, glucose, and bone metabolism [17]. Previous studies on physiological ovarian aging have demonstrated changes in lipid, amino acid, and indoleacetic acid metabolism in perimenopausal women, highlighting potential cardiovascular and metabolic risks [18, 19].

In the context of pathological ovarian aging, metabolomic studies have uncovered specific alterations. Liang et al. [20] linked oxylipin metabolites and arachidonic acid (AA) metabolic pathway with oocyte development. Oxylipins could be produced by the autooxidation of AA, and AA is essential for oocyte maturation, development and fertility [21]. Moreover, a recent plasma metabolomics study identified lipids such as arachidonoyl amide, 18-hydroxyeicosatetraenoic acid (HETE), and phosphoglyceride (PG) (16:0/18:1) as biomarkers with potential for diagnosing POI [22]. Another study found that POR women with decreased AMH levels showed downregulated serum prostaglandin H2, cortisone, and tetracosanoic acid [23]. Despite these findings, the distinction between physiological and pathological ovarian aging remains unclear.

While metabolomics provides dynamic insights into both physiological and pathological changes, few studies have examined the progression of ovarian aging over time. A long-term study [24] revealed that women experiencing rapid declines in anti-Müllerian hormone (AMH) levels exhibited higher serum concentrations of metabolites such as phosphate, N-acetyl-D-glucosamine, branched chained amino acids (BCAAs), proline, urea, and pyroglutamic acid.

In this study, we employed untargeted metabolomics to investigate differential serum metabolites associated with both physiological and pathological ovarian aging. We further explored homogeneity and heterogeneity in metabolic characteristics between the two forms of aging. Our findings contribute to a deeper understanding of the mechanisms underlying ovarian aging and provide valuable insights for clinicians to improve the diagnosis and prevention of this condition.

Materials and methods

Participants and sample collection

Serum samples were collected from 70 participants at the First Affiliated Hospital, Guangzhou University of Chinese Medicine (Guangzhou, China), between March 2022 and October 2022. The participants were grouped as follows: 13 women with physiological ovarian aging (old), 12 with DOR, 14 with scPOI, 19 with POI, and 12 healthy women (control, Ctrl). This study was approved by the Ethics Committee of First Affiliated Hospital of Guangzhou University of Chinese Medicine (No. JY2022-002), and is in accordance with the Declaration of Helsinki. Informed consent was obtained from all the participants prior to sample collection. The inclusion criterion for the old group was (1) age \geq 45 years;

(2) without the history of diminished ovarian function. DOR, scPOI, and POI are different stages of pathological ovarian aging. Considering the complex diagnostic criteria of DOR and the overlap of DOR and scPOI [25, 26], inclusion criteria of pathological ovarian aging were set as below: (1) age 20–40 years old; (2) AMH < 1.1 ng/mL and basic follicle-stimulating hormone (bFSH) < 15 mIU/mL (DOR), $15 \leq \text{bFSH} < 25$ mIU/mL (scPOI), $\text{bFSH} \geq 25$ mIU/mL (POI). Participants who met the following criteria were excluded from the study: (1) diagnosis of other endocrine diseases, such as polycystic ovarian syndrome, hyperprolactinemia, or thyroid dysfunction; (2) diagnosis of ovarian endometriosis; (3) hormone or ovarian stimulation treatment in the past 3 months; and (4) history of oophorectomy. The participants' characteristics are shown in Table 1. Serum was collected on the 2nd or 3rd day of menstruation. In cases of amenorrhea or menopause, serum was collected randomly. Then serum samples were stored at -80°C .

Pre-treatment of serum samples

Serum samples were thawed at 4°C . Then, 100 μL of serum was resuspended with 400 μL of 80% methanol using well vortex. After sonicating for 5 min in an ice-water bath, the serum samples were centrifuged at $15,000 \times g$, 4°C for 20 min. The supernatant was diluted with water to a final concentration containing 53% methanol. After centrifuging at $15,000 \times g$, 4°C for 20 min, 140 μL of the supernatant was collected for further analysis. Additionally, 2 μL of each sample was mixed for quality

control (QC). Additionally, same reagent but without serum was defined as blank sample and tested.

Ultra-high performance liquid chromatography-tandem mass spectrometry (UPLC-MS/MS) analysis

UHPLC-MS/MS analysis was performed using a Vanquish UPLC system (Thermo Fisher Scientific) coupled with an Orbitrap Q Exactive™ HF mass spectrometer (Thermo Fisher Scientific). Chromatographic separation was performed on a ThermoFisher Hypersil Gold C18 column (100×2.1 mm, $1.9 \mu\text{m}$) at 40°C . Precisely 0.1% (v/v) formic acid (A) and methanol (B) were used as mobile phases for positive-ion-mode, and 5 mM ammonium acetate (pH=9.0, A) and methanol (B) were used as mobile phases for negative-ion mode. The flow rate was 0.2 mL/min. After equilibration, 5 μL of each sample was injected, and the flowing gradient elution was as below: 2% B from 0 to 1.5 min, 2–85% B from 1.5 to 3 min, 85–100% B from 3 to 10 min, 100–2% B from 10 to 10.1 min, 2% B from 10.1 to 11 min, and 2% B from 11 to 12 min.

Mass spectrometry analysis was performed in both positive- and negative-ion modes. The source ionization parameters were set as below: spray voltage = 3500 V; sheath gas flow rate = 35 psi; aux gas flow rate = 10 mL/min; capillary temperature = 320°C ; aux gas heater temperature = 350°C . Data were acquired over the m/z range of 100–1500.

To removing the background noise, the blank sample was injected before injecting serum samples. To confirm the stability and repeatability of the system, samples

Table 1 Characteristics of participants

Item	ctrl (n = 12)	old (n = 13)	DOR (n = 12)	scPOI (n = 14)	POI (n = 19)
Age (years)	30.17 ± 5.65	51.85 ± 3.39***	33.42 ± 3.15	32.21 ± 6.78	32.89 ± 7.45
BMI (kg/m ²)	21.63 ± 0.86	22.70 ± 1.71	21.17 ± 1.18	22.13 ± 0.96	21.29 ± 1.24
Age at menarche (years)	12.92 ± 0.67	13 ± 0.58	13.08 ± 0.67	13.07 ± 0.73	12.95 ± 0.71
Gravidity	1.5 (0, 2.75)	3 (2, 4)*	2 (0.25, 3)	2 (0.75, 2.25)	2 (0, 3)
Parity	1 (0, 1)	2 (1, 2.5)**	1 (0.25, 2)	1 (0, 2)	0 (0, 2)
pregnancy loss	0 (0, 0)	0 (0, 1)	0 (0, 0.75)	0 (0, 0)	0 (0, 0)
Diabetes (n(%))	0 (0%)	0 (0%)	0 (0%)	0 (0%)	0 (0%)
Cardiovascular disease (n(%))	0 (0%)	0 (0%)	0 (0%)	0 (0%)	0 (0%)
Hormones					
bFSH (mIU/mL)	5.26 ± 0.98	54.72 ± 26.00***	10.05 ± 2.75***	19.4 ± 2.78***	67.27 ± 28.7***
bLH (mIU/mL)	4.92 ± 1.18	38.65 ± 18.09***	5.66 ± 2.36*	8.26 ± 3.46	34.76 ± 20.58***
bFSH/bLH	1.13 ± 0.36	1.49 ± 0.53	2.06 ± 1.01*	2.84 ± 1.51***	2.17 ± 0.74***
bE ₂ (pmol/L)	185.67 ± 53.69	74.97 ± 53.59**	188.66 ± 162.76	165.36 ± 82.27	74.73 ± 40.76***
bT (nmol/L)	0.74 ± 0.39	0.37 ± 0.23	0.63 ± 0.37	0.35 ± 0.27*	0.48 ± 0.29
AMH (ng/mL)	3.90 ± 1.88	0.01 ± 0.01***	0.43 ± 0.38***	0.33 ± 0.51***	0.03 ± 0.04***
Lifestyles					
Smoking (n(%))	1 (8.33%)	2 (15.38%)	1 (8.33%)	0	1 (5.26%)
Coffee (n(%))	1 (8.33%)	1 (7.69%)	1 (8.33%)	0	0
Tea (n(%))	0	1 (7.69%)	0	0	1 (5.26%)

Comparing to the Ctrl group, * $P < 0.05$, ** $P < 0.01$, *** $P < 0.001$. Ctrl: control; BMI: body mass index; bFSH: basic follicle-stimulating hormone; bLH: basic luteinizing hormone; bE₂: basic estradiol; bT: basic testosterone; AMH: anti-Müllerian hormone

were injected randomly, and QC samples were repeatedly injected after injecting eight samples.

Data collection and processing

Raw data were processed using Compound Discoverer (Version 3.1, Thermo Fisher Scientific) to perform peak alignment, peak picking, metabolite identification, and quantification. Parameters for peak alignment and picking were set as below: retention time tolerance ± 0.2 min; actual mass tolerance ± 5 ppm; signal intensity tolerance $\pm 30\%$; signal to noise ratio ≥ 3 (when signal to noise ratio ≤ 3 , peaks would be defined as background). The molecular weight was determined based on m/z , the molecular formula was predicted based on ppm and additive ions, then automatically matched with mzCloud (<https://www.mzcloud.org/>), mzVault (Version 2.3, local database) and Masslist (local database) for MS1 analysis [25, 26]. Further, MS2 analysis were made by automatically matching the molecular ions, fragment ions and collision energy in mzCloud and mzVault databases. Then identified metabolites were annotated by The Kyoto Encyclopedia of Genes and Genomes (KEGG, <https://www.genome.jp/kegg/pathway.html>), The Human Metabolome Database (HMDB, <https://hmdb.ca/metabolites>) and LIPID MAPS (<https://www.lipidmaps.org/>). Compound classes were obtained from these databases. Normalized quantification results were obtained according to the QC-based method: raw metabolite quantification of each sample / (sum of raw metabolite quantification/sum of metabolite quantification of QC sample).

Statistical analysis

Data were statistically analyzed using SPSS software (version 26.0). Continuous variables with normal distributions were described as mean \pm standard deviation (SD) and analyzed using one-way analysis of variance (ANOVA). For parametric ANOVA, Dunnett was used in multiple comparison test; For variables without normal distribution or multiple comparison test with unequal variances, Kruskal-Wallis H test was used. Spearman's rank correlation test was performed for the correlation analysis. $P < 0.05$ was considered statistically significant.

MetaX software (<http://metax.genomics.cn>) was used to perform multivariate analysis, including principal component analysis (PCA) and orthogonal projections to latent structure discriminant analysis (OPLS-DA). Variable importance in the projection (VIP) of OPLS-DA was determined. Between groups, metabolites with variable importance in projection (VIP) > 1 , fold change (FC) > 1.5 or < 0.667 , and $P < 0.05$ were recognized as differential metabolites. Moreover, the validation of the OPLS-DA model was assessed by 7-fold cross-validation (the model was considered validated especially when R^2Y were close to 1) and a permutation test (the model was considered

validated when $R^2 > Q^2$ and $Q^2 < 0$). The correlation between differential metabolites was calculated using the R language (Version 4.0). KEGG databases was used for metabolic pathway enrichment analysis. $P < 0.05$ was considered statistically significant.

Results

Clinical characteristics of participants

Significant clinical characteristics, including age, body mass index (BMI), menstruation / pregnancy / metabolic disease histories, hormone levels and lifestyles, were collected and shown in Table 1. The differences between groups were mainly focus on the hormones.

Compared to the control group, bFSH levels in the old, DOR, scPOI, and POI groups were significantly increased to various degrees ($P < 0.001$). Accordingly, the AMH levels in these groups significantly decreased to various degrees ($P < 0.001$). The basic luteinizing hormone (bLH) levels significantly increased in the old, DOR, and POI groups. However, a bFSH/bLH ratio > 2 was only observed in the DOR ($P < 0.05$), scPOI ($P < 0.001$), and POI groups ($P < 0.001$), which may represent a new difference between physiological and pathological ovarian aging. Additionally, decreased baseline estradiol (bE_2) levels were observed in the old ($P < 0.01$) and POI groups ($P < 0.001$), and scPOI group showed a significant decrease in baseline testosterone (bT) levels ($P < 0.05$). In summary, these serum hormone levels indicate diminished ovarian function during physiological and pathological ovarian aging.

Multivariate analysis of metabolites

After relative standard deviation denoising, 448 and 325 metabolites were identified in the positive-ion and negative-ion modes, respectively. The unsupervised PCA of all groups showed a similar distribution of variations, especially in the scPOI and POI groups (Fig. 1B; Supplementary Fig. 1A). Unlike the other ovarian aging groups, variations in the DOR group were more similar to those in the control group. Further PCA of each ovarian aging group and the control group was performed, which showed distinct separation tendencies (Fig. 1C, E, I, L; Supplementary Fig. 1B, E, H, K).

Supervised OPLS-DA was applied to maximize group separation and identify discriminating metabolites, which showed marked improvements in group separation (Fig. 1D, G, J, M; Supplementary Fig. 1C, E, I, L; Supplementary Fig. 2B, E, H, K, N, Q; Supplementary Fig. 3B, E, H, K, N, Q). 7-fold cross-validation of OPLS-DA models showed R^2Y (0.926–0.986) and Q^2Y (0.38–0.826). Two hundred random permutation tests showed that $R^2 > Q^2$ and Q^2 intercepting the Y axis at $-0.5 \sim -1.0$ (Fig. 1E, H, K, N; Supplementary Fig. 1D, G, J, M; Supplementary Fig. 2C, F, I, L, O, R; Supplementary Fig. 3C, E, I, L, O,

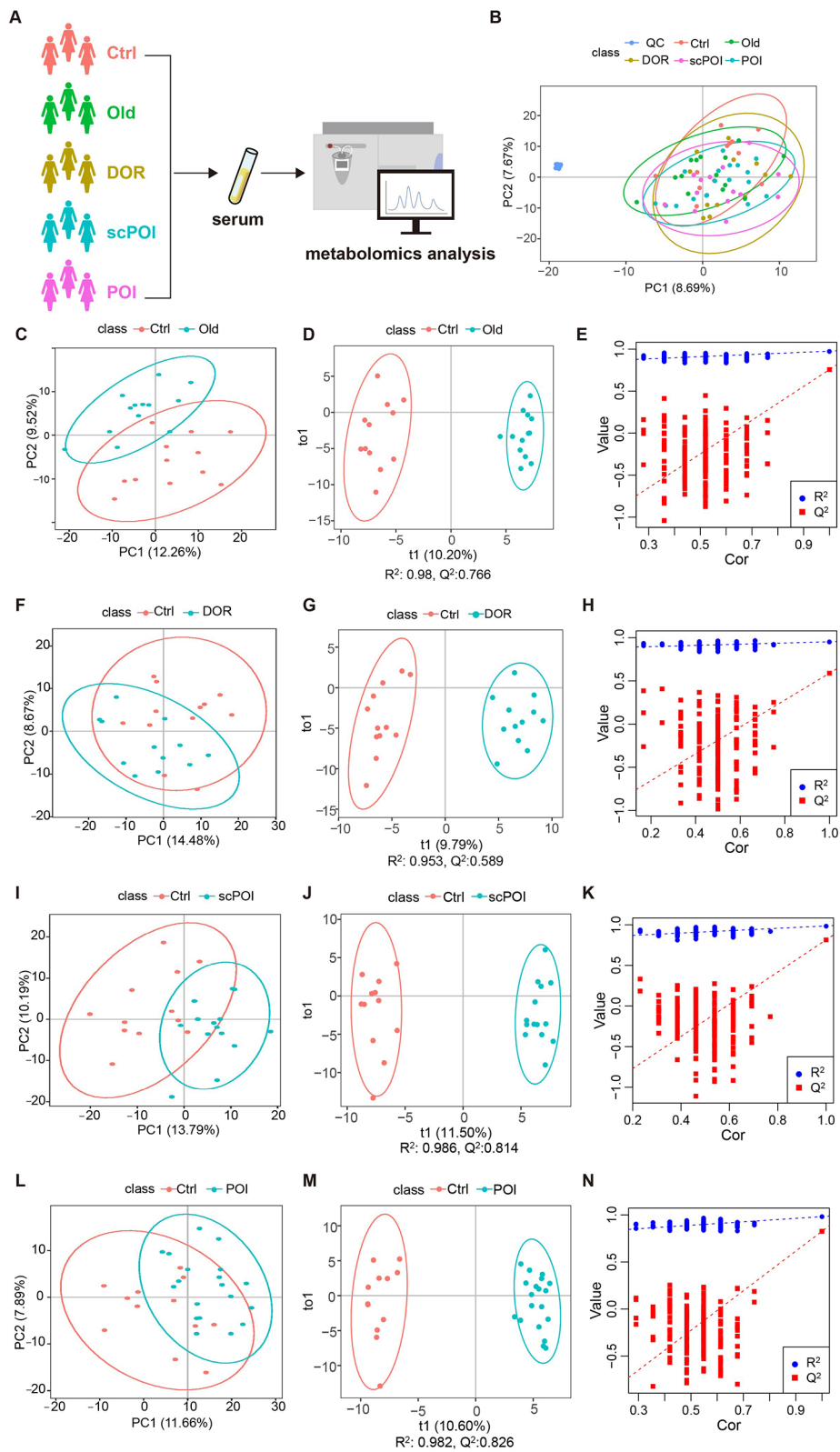


Fig. 1 (See legend on next page.)

(See figure on previous page.)

Fig. 1 Principal component analysis (PCA) score plots, orthogonal projections to latent structure discriminant analysis (OPLS-DA) score plots and corresponding validation plots in ESI⁺ mode. **(A)** The workflow of the study. PCA score plots of all groups **(B)**, control ($n = 12$) and old ($n = 13$) groups **(C)**, control and DOR ($n = 12$) groups **(F)**, control and scPOI ($n = 14$) groups **(I)**, control and POI ($n = 19$) groups **(L)**. OPLS-DA score plots of control and old groups **(D)**, control and DOR groups **(G)**, control and scPOI groups **(J)**, control and POI groups **(M)**. Permutation test of OPLS-DA model in control and old groups **(E)**, control and DOR groups **(H)**, control and scPOI groups **(K)**, control and POI groups **(N)**. Ctrl: control. DOR: diminished ovarian reserve. scPOI: subclinical premature ovarian insufficiency. POI: premature ovarian insufficiency

R). These data indicated stable and not overfitting OPLS-DA models. The OPLS-DA results demonstrated significant metabolic differences between the participants with ovarian aging and healthy participants, the participants with physiological ovarian aging and pathological ovarian aging, and the participants with different pathological ovarian aging.

Identification of significant differential metabolites in physiological and pathological ovarian aging

Given the success of the OPLS-DA model in classifying the ovarian aging groups and the control group, significant differential metabolites from positive-ion and negative-ion modes were integrated and are shown in volcano plots. Compared to the control group, metabolites marked with bright red color were significantly upregulated in the ovarian aging groups, and metabolites marked with bright blue color were significantly downregulated in the ovarian aging groups. Overall, 20, 26, 18 and 21 differential metabolites were identified in the old vs. control group (Fig. 2A), DOR vs. control group (Fig. 2B), scPOI vs. control group (Fig. 2C), and POI vs. control group (Fig. 2D), respectively.

The top10 differential metabolites ($|\log_2FC|$ value-based) were yellow-marked and showed in Supplementary Table 1. We then clustered these significant differential metabolites into groups (Fig. 2E), menaquinone, neopterin and SM (d22:1/14:1) were clustered. Interestingly, these metabolites were significantly downregulated both in physiological and pathological ovarian aging groups. Alpha-benzylsuccinic acid and SM (d27:0/14:1) were clustered and significantly upregulated in the old group. In the pathological ovarian aging groups, SM (d17:0/25:1), 9-[(2-hydroxyethoxy)methyl]-1,9-dihydro-6 H-purin-6-one and 15-deoxy- Δ 12,14-prostaglandin A1 were clustered and significantly upregulated in the DOR group, while taurocholic acid and SM (d14:0/20:2) were clustered and significantly downregulated. Tetranor-12(R)-HETE, (+/-)8(9)-DIHET and 3-methoxytyramine were clustered and significantly upregulated in the scPOI group but significantly downregulated in the POI group.

Homogeneity and heterogeneity between physiological and pathological ovarian aging

To further explore the homogeneity of physiological and pathological ovarian aging, significant differential

metabolites identified in the old vs. control group, DOR vs. control group, scPOI vs. control group, and POI vs. control group were compared using a venn diagram (Fig. 3A). Five metabolites have been recognized to be common in physiological and pathological ovarian aging. Among these metabolites, neopterin (Fig. 3B, $P < 0.05$), menaquinone (Fig. 3C, $P < 0.01$), SM (d14:1/24:2) (Fig. 3E, $P < 0.01$) and SM (d14:0/21:1) (Fig. 3F, $P < 0.05$) were significantly downregulated both in the physiological and pathological ovarian aging groups. SM (d17:0/25:1) (Fig. 3D, $P < 0.01$) was significantly upregulated both in the physiological and pathological ovarian aging groups.

Among these common metabolites, only downregulated extent of SM (d14:0/21:1) both in physiological and pathological ovarian aging showed no difference. Directly comparing with the old group, neopterin ($P < 0.05$) and menaquinone ($P < 0.01$) in the POI group showed a larger extent of downregulation, while SM (d17:0/25:1) in the DOR group showed a higher extent of upregulation ($P < 0.05$). Additionally, downregulation of SM (d14:1/24:2) in all pathological ovarian aging groups was less than that in the physiological ovarian aging group ($P < 0.05$). In the pathological ovarian aging groups, upregulated extent of SM (d17:0/25:1) in the DOR group was higher than those in the scPOI ($P < 0.01$) and POI groups ($P < 0.05$).

Differential metabolites specifically changed in the physiological ovarian aging group were further studied (Supplementary Table 2). Testosterone sulfate (Fig. 3G, $P < 0.001$), PC (16:0/19:2) (Fig. 3J, $P < 0.01$) and PC (18:2/19:2) (Fig. 3K, $P < 0.05$) were significantly downregulated. While alpha-benzylsuccinic acid (Fig. 3H, $P < 0.05$), C-8 ceramide-1-phosphate (Fig. 3I, $P < 0.05$) and PC (16:2e/20:0) (Fig. 3L, $P < 0.05$) were significantly upregulated.

Among these metabolites, testosterone sulfate level in the old group was also lower than those in the DOR ($P < 0.001$) and POI group ($P < 0.01$). PC (16:0/19:2) in the old group was downregulated when comparing to the control group, but the level was still higher when comparing to the scPOI group ($P < 0.05$). In those three physiological ovarian aging specifically upregulated metabolites, alpha-benzylsuccinic acid level in the old group was also higher than those in the DOR group ($P < 0.05$) and the POI group ($P < 0.01$), C-8 ceramide-1-phosphate level in the old group was also higher than those in the DOR group ($P < 0.001$) and the scPOI group

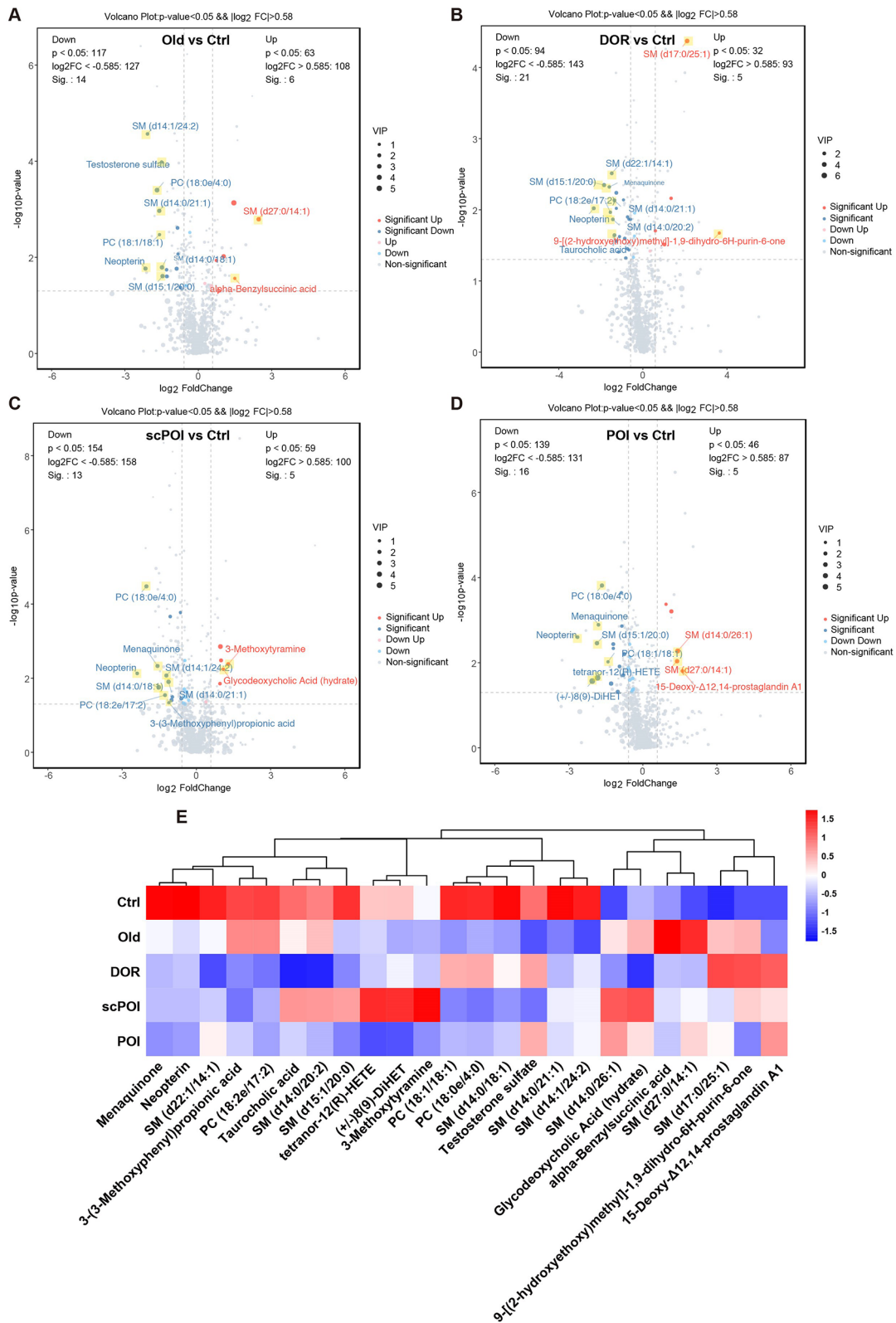


Fig. 2 The identification of differential metabolites. Volcano plot shows the differential metabolites between old and control groups (A), DOR and control groups (B), scPOI and control groups (C), POI and control groups (D). Comparing to the control group, the up-regulated and down-regulated metabolites were marked in red and blue, respectively. (E) The heatmap analyzes hierarchical clustering of the top 10 differential metabolites in all groups

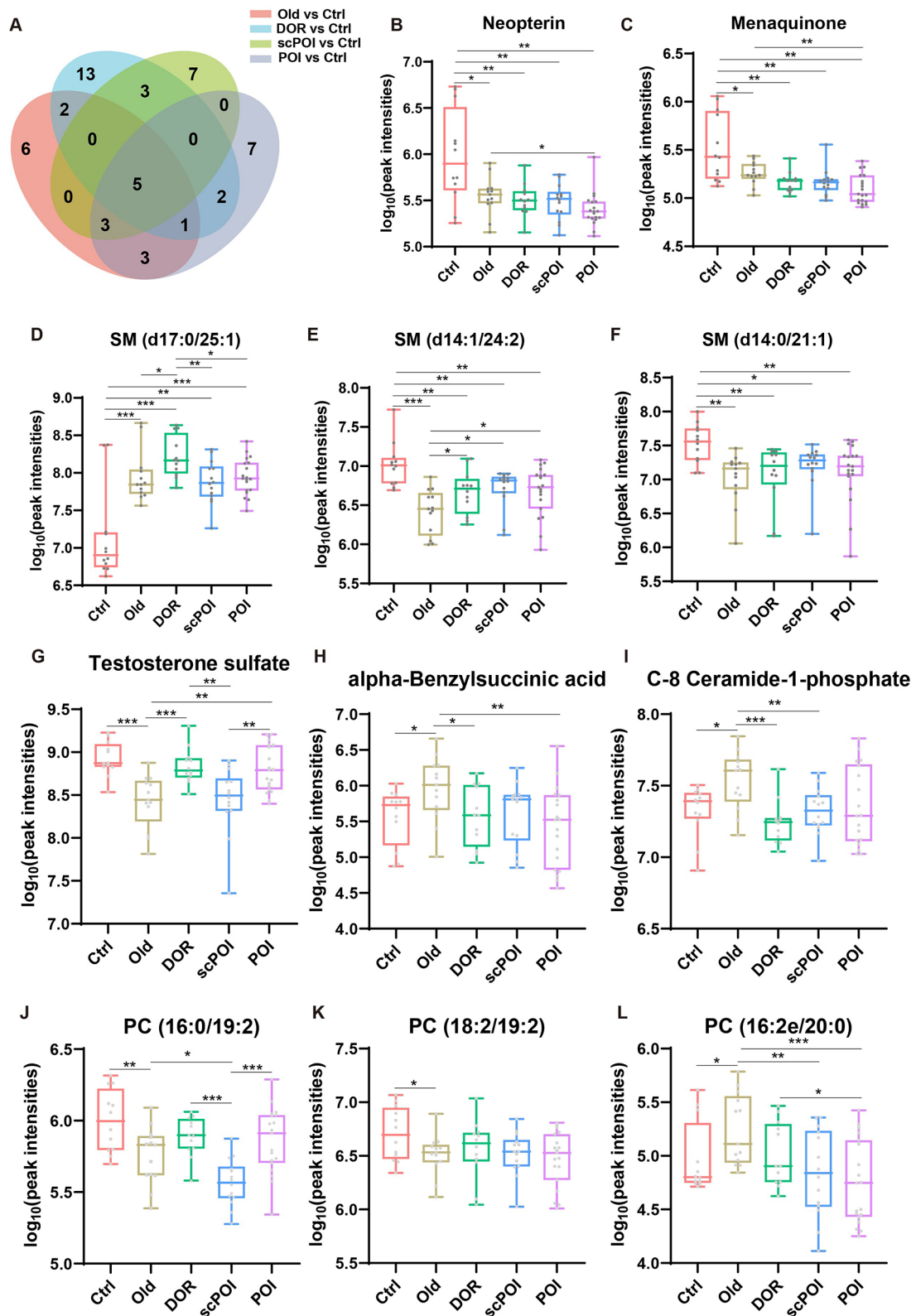


Fig. 3 The identification of common aging metabolites between physiological and pathological ovarian aging, physiological ovarian aging-specific metabolites. **(A)** Venn plot shows the differential metabolites in all groups. And there are five common aging metabolites between physiological and pathological ovarian aging **(B-F)**. **(G-L)** The physiological ovarian aging-specific metabolites. * $P < 0.05$, ** $P < 0.01$, *** $P < 0.001$

($P < 0.01$), PC (16:2e/20:0) level in the old group was also higher than those in the scPOI group ($P < 0.01$) and the POI group ($P < 0.001$).

The correlation between differential metabolites reflects synergistic or repulsive effects on functional regulation. Pearson correlation coefficient analysis was performed in the physiological ovarian aging differential metabolites (Supplementary Fig. 4A). Results showed that menaquinone, one of the common differential metabolites, was positively correlated with neopterin ($P < 0.001$). Testosterone sulfate, one of the physiological ovarian aging specific differential metabolites, was positively correlated with SM (d15:1/20:0) ($P < 0.001$), but negatively correlated with PC (16:2e/20:0) ($P < 0.05$).

Homogeneity and heterogeneity between different stages of pathological ovarian aging

Based on the venn diagram analysis (Figs. 3A and 4A), we further compared the homogeneity and heterogeneity between three pathological ovarian aging groups. The results showed that the PC (17:0/18:2) (Fig. 4B, $P < 0.05$), PC (18:2e/17:2) (Fig. 4C, $P < 0.05$) and SM (d22:1/14:1) (Fig. 4D, $P < 0.05$) were significantly downregulated both in the DOR and scPOI groups. And downregulated extents of these three metabolites both in the DOR group and scPOI group showed no difference. When directly comparing to the old group, PC (17:0/18:2) level in the POI group ($P < 0.01$), PC (18:2e/17:2) level and SM (d22:1/14:1) level in the DOR group were significantly lower ($P < 0.05$).

SM (d14:1/20:1) (Fig. 4E, $P < 0.05$) and 4-hydroxyretinoic acid (Fig. 4F, $P < 0.05$) were significantly downregulated both in the DOR and POI groups, and 4-hydroxyretinoic acid level in the POI group showed a higher downregulation extent ($P < 0.001$). Although downregulation extents of SM (d14:1/20:1) showed no difference between the DOR and POI groups, SM (d14:1/20:1) levels in these two groups were significantly lower than that in the scPOI group ($P < 0.01$).

As for the pathological ovarian aging specific metabolites, 9-[(2-hydroxyethoxy)methyl]-1,9-dihydro-6 H-purin-6-one was specifically upregulated in the DOR group ($P < 0.05$), 3-(3-methoxyphenyl)propionic acid was specifically downregulated in the scPOI group ($P < 0.05$), and vitamin A was specifically downregulated in the POI group ($P < 0.05$). When comparing to the old group, 3-(3-methoxyphenyl)propionic acid levels in pathological ovarian aging groups were significantly lower ($P < 0.01$).

Pearson correlation coefficient analysis (Supplementary Fig. 4B) of ten common differential metabolites of pathological ovarian aging showed that menaquinone, one of the common differential metabolites, was positively correlated with 4-hydroxyretinoic acid ($P < 0.05$). SM

(d22:1/14:1), one of the common differential metabolites of the DOR and scPOI groups, was positively correlated with menaquinone ($P < 0.001$) but negatively correlated with SM (d17:0/25:1) ($P < 0.01$).

Metabolic pathways associated with physiological and pathological ovarian aging

KEGG pathway analysis was performed to investigate enriched metabolic pathways associated with physiological and pathological ovarian aging. Significant differential metabolites in both physiological and pathological ovarian aging were mainly enriched in folate biosynthesis, ubiquinone and other terpenoid-quinone biosynthesis (Fig. 5A-D, $P < 0.05$). Other metabolic pathways were also enriched in pathological ovarian aging groups. Significant differential metabolites in the scPOI group were enriched in dopaminergic synapses pathway ($P < 0.05$). Significant differential metabolites in the POI group were also mainly enriched in vitamin digestion and absorption and retinol metabolism ($P < 0.05$).

Predictive value of typical metabolites on physiological and pathological ovarian aging

ROC curve analysis was used to assess the predictive value of differential metabolites for ovarian aging. In physiological ovarian aging, testosterone sulfate showed high predictive value with an area under the curve (AUC) of 0.929 (95% CI: 0.82–1, Youden's index: 0.84) (Fig. 6A), indicating that decreased serum testosterone sulfate levels could predict physiological ovarian aging. In pathological ovarian aging, increased levels of SM (d14:0/28:1), PC (18:0e/4:0) and 4-hydroxyretinoic acid showed high sensitivity and specificity for DOR, scPOI, and POI (Fig. 6B-D), respectively. The AUC of these markers were 0.847 (95% CI: 0.563–1, Youden's index: 0.763), 0.923 (95% CI: 0.81–1, Youden's index: 0.762), and 0.921 (95% CI: 0.822–1, Youden's index: 0.789), respectively. These new markers showed nearly equal predictive values compared to accepted markers bFSH and AMH (AUC = 1).

The predictive value of five common metabolites in pathological ovarian aging were also analyzed. Result showed that PC (17:0/18:2), SM (d22:1/14:1) and 4-hydroxyretinoic acid showed highest predictive values for POI with an AUC of 0.851, 0.921 and 0.921 (Supplementary Fig. 5A, C, E). PC (18:2e/17:2) and SM (d14:1/20:0) showed highest predictive values for DOR with an AUC of 0.799 and 0.743 (Supplementary Fig. 5B, D). Additionally, combining these five metabolites also showed high predictive values for pathological ovarian aging with the AUC > 0.900 (Supplementary Fig. 5F).

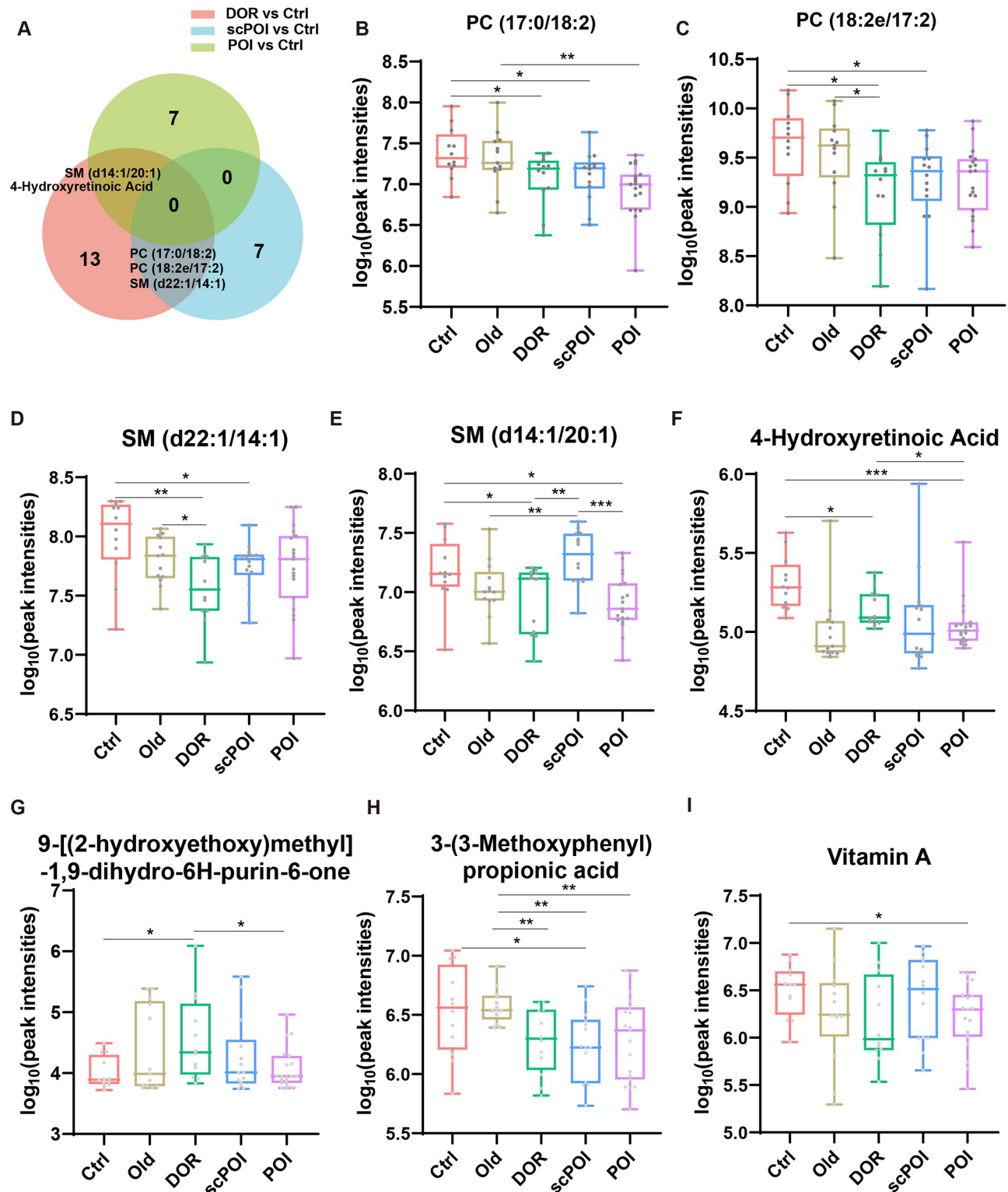


Fig. 4 The identification of common aging metabolites in pathological ovarian aging. **(A)** Venn plot shows the common metabolites in three pathological ovarian aging groups. **(B-F)** There are five common aging metabolites in pathological ovarian aging. **(G-I)** The examples of DOR, scPOI or POI-specific aging metabolites. * $P < 0.05$, ** $P < 0.01$, *** $P < 0.001$

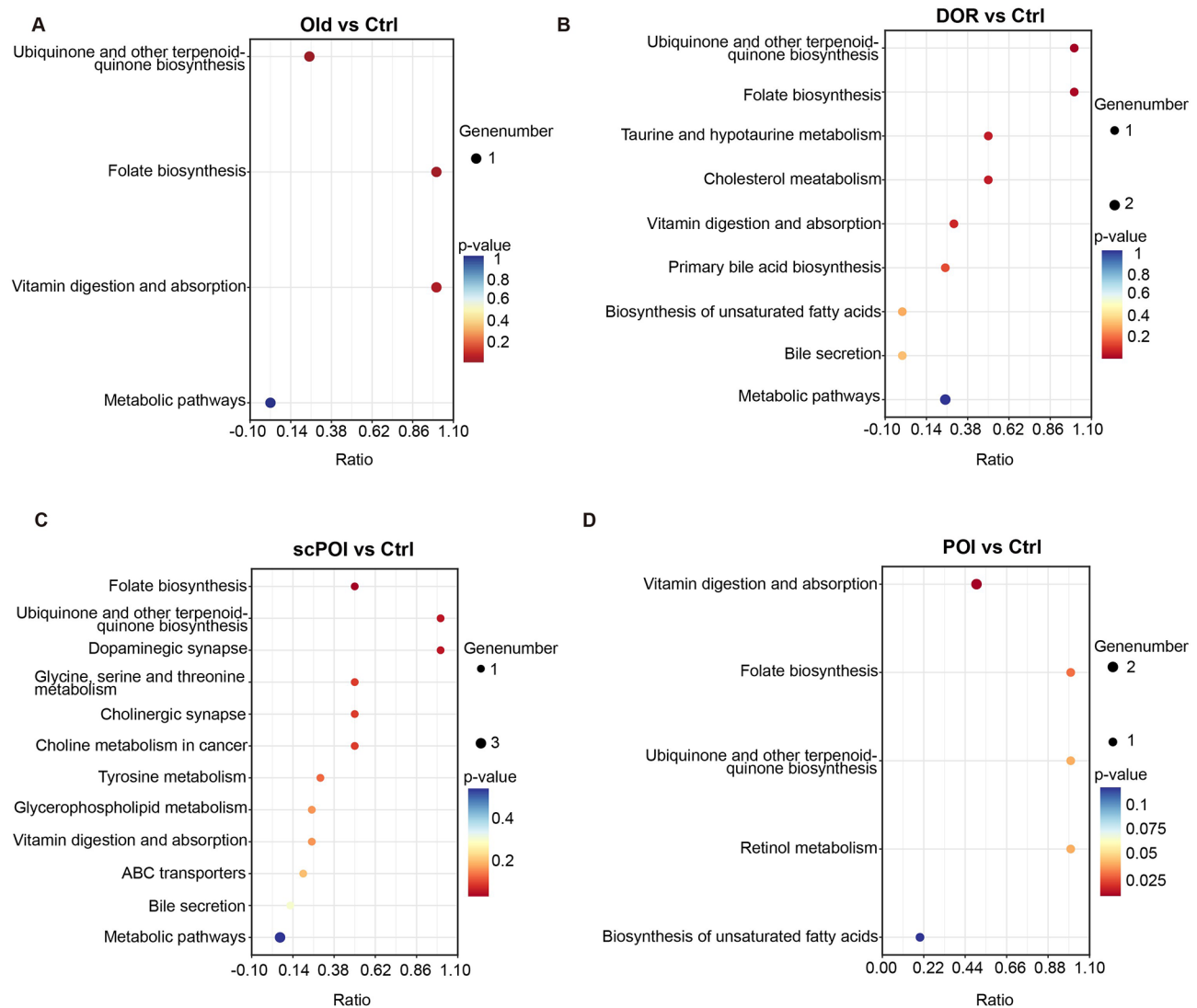


Fig. 5 Metabolic pathways in physiological and pathological ovarian aging. Bubble plots show the KEGG pathways enriched with differential metabolites between the old and control groups (A), the DOR and control groups (B), the scPOI and control groups (C), the POI and control groups (D)

Correlation analysis of common differential metabolites and significant clinical parameters

To further investigate the credibility of significant differential metabolites in predicting ovarian aging, Spearman's correlation analyses were performed between five common metabolites of physiological and pathological ovarian aging, five common metabolites of pathological ovarian aging, and diagnostic standards (age, bFSH, and AMH, Table 2). SM (d14:1/24:2) ($P < 0.01$), 4-hydroxyretinoic acid ($P < 0.01$) and SM (d14:0/21:1) ($P < 0.05$) negatively correlated with age.

Neopterin ($P < 0.05$), menaquinone ($P < 0.05$), SM (d14:1/24:2) ($P < 0.05$), 4-Hydroxyretinoic Acid ($P < 0.001$) and SM (d14:1/20:1) ($P < 0.05$) were negatively correlated with bFSH. Menaquinone ($P < 0.05$), SM (d14:1/24:2) ($P < 0.01$), SM (d14:0/21:1) ($P < 0.05$) and

4-hydroxyretinoic acid ($P < 0.001$) were positively correlated with AMH.

Combining the correlation results with diagnostic standards, SM (d14:1/24:2) showed strong correlations with both physiological and pathological ovarian aging. Additionally, 4-hydroxyretinoic acid levels strongly correlated with pathological ovarian aging.

Discussion

Decreased fertility rates, various complications, and poor quality of life related to ovarian aging are critical issues. Discovering reliable biomarkers to assess ovarian aging and developing safe drugs to prevent and cure ovarian aging have become significant challenges for promoting healthy aging [27]. In this study, we investigated the metabolic characteristics of both physiological and pathological ovarian aging and found five common differential

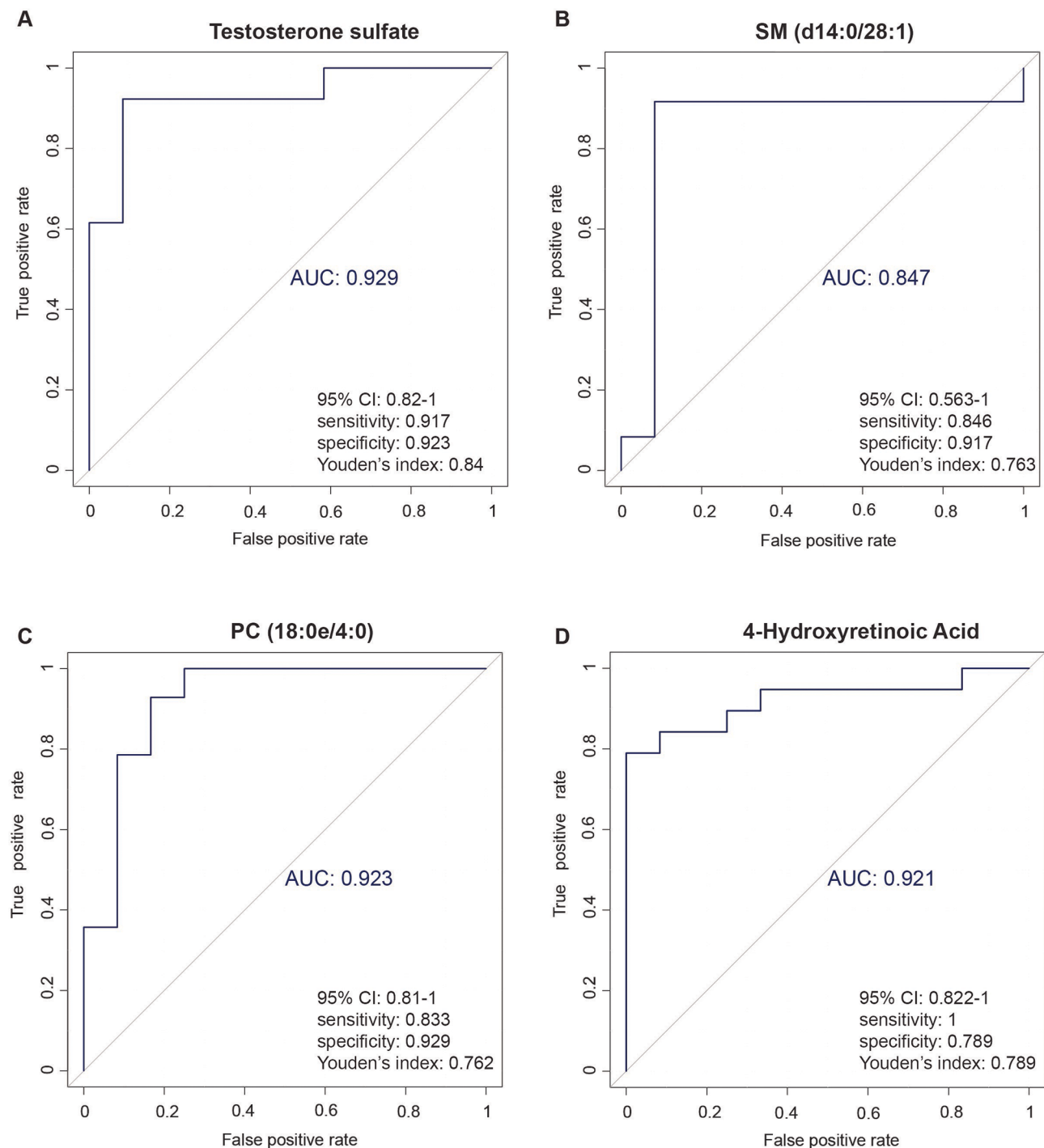


Fig. 6 ROC analysis of metabolites in physiological and pathological ovarian aging. ROC curves show the clinical significance of testosterone sulfate in the old group (A), SM (d14:0/28:1) in the DOR group (B), PC (18:0e/4:0) in the scPOI group (C) and 4-hydroxyretinoic acid in the POI group (D)

metabolites of ovarian aging and five specific differential metabolites of pathological ovarian aging. Metabolic pathways, such as folate biosynthesis, ubiquinone and other terpenoid-quinone biosynthesis pathways, are mainly involved both in physiological and pathological ovarian aging. While dopaminergic synapses, vitamin

digestion and absorption and retinol metabolism, were specifically associated with pathological ovarian aging. We also found that several metabolites, including testosterone sulfate, SM (d14:0/28:1), PC (18:0e/4:0) and 4-hydroxyretinoic acid showed a close correlation with ovarian aging and could be new biomarkers in diagnosing

Table 2 Correlation analysis between the concentration of metabolites with age, basic FSH (bFSH) and AMH level

Metabolites	Age	bFSH	AMH
Neopterin	0.1	-0.30*	0.22
Menaquinone	0.05	-0.30*	0.28*
SM (d17:0/25:1)	0.15	0.21	-0.18
SM (d14:1/24:2)	-0.34**	-0.29*	0.35**
SM (d14:0/21:1)	-0.24*	-0.21	0.26*
SM (d22:1/14:1)	-0.23	-0.09	0.13
PC (18:2e/16:0)	0.04	0.11	-0.21
PC (17:0/18:2)	0.02	-0.18	0.12
4-Hydroxyretinoic Acid	-0.33**	-0.46***	0.58***
SM (d14:1/20:1)	-0.20	-0.30*	0.23

* $P < 0.05$, ** $P < 0.01$, *** $P < 0.001$. - were found to be negatively correlated

of physiological ovarian aging, DOR, scPOI and POI, respectively.

The homogeneity between physiological and pathological ovarian aging could reflect the essence of ovarian aging. In this study, the majority of common differential metabolites were SM and PC. They are not only fundamental structural elements of cell membranes but also key molecules in regulating energy metabolism and signal transduction. In the ovarian aging groups, SM (d17:0/25:1) was significantly increased, whereas SM (d14:1/24:2) and SM (d14:0/21:1) were significantly decreased. In particular, SM (d14:1/24:2) was significantly and negatively correlated with ovarian aging. The sphingosine base is a common structure in sphingolipids. Sphingosine with a longer chain appears to be positively correlated with ovarian aging. Longer chains would cause lower water solubility and decreased cell membrane mobility [28, 29]. In contrast, sphingolipids, including SM, accumulate linearly with age, and although these accumulations are necessary for early development, they may promote age-related diseases by increasing reactive oxygen species or inhibiting Bcl-2 [30, 31]. Another lipid, menaquinone, was significantly decreased in the ovarian aging group. Menaquinones (also known as vitamin K2), enriched in ubiquinone and other terpenoid-quinone biosynthesis pathway, are a family of redox-active small molecules that are crucial for energy production in bacteria and the post-translational γ -carboxylation of some proteins [32]. Menaquinone deficiency not only impairs blood coagulation but also leads to age-related diseases such as Alzheimer's disease and osteoporosis. Supplementation with menaquinone can reverse structural and cognitive deterioration by regulating the nucleotide-binding oligomerization domain-like receptor protein 3 (NLRP3)/caspase-1/Nrf-2 signaling pathway [33], promote bone mineralization, and indirectly increase bone strength [34]. However, the effect of menaquinone on ovarian aging remains unclear. In addition to lipids, lower neopterin levels were observed in the ovarian aging

groups. Neopterin, enriched in folate biosynthesis pathway, is a metabolite of guanosine-5'-triphosphate (GTP) and is recognized as a marker of macrophage activation. Contrary to our study, previous studies [35, 36] showed that neopterin level was positively associated with age. During aging, the number of cells, including macrophages, decreases. However, age-related chronic inflammation occurs as immunity decreases. A previous study [37] found that old mice showed an increased frequency of C-X-C Motif Chemokine Receptor 3 (CX3CR1) expressing macrophage and a reduction in Ly6C⁺ macrophages, which suggested that macrophages would adopt a more immunosuppressive phenotype. Additionally, the homogeneity of physiological and pathological ovarian aging is reflected in folate biosynthesis. Neopterin is the end product of pterin metabolism, and folate is required to form the starting molecule for pterin metabolism. Folate showed a strong positive association with neopterin concentration in older people with depression [38]. Folate is essential for oocyte development, as it is taken up by reduced folate carrier (RFC1) and folate receptor 1 (FOLR1), both of which are highly expressed in cumulus-oocyte complexes (COC) and oocytes. Folate deficiency can impair the activation of the TGF β 1/Smad signaling pathway, which in turn disrupts autophagy and reduces ROS scavenging ability, contributing to ovarian dysfunction [39–40]. Additionally, folate acts as an important methyl donor; folate deficiency can disrupt DNA methylation patterns, leading to gene expression alterations, base substitutions, DNA breaks, and gene deletions within follicles [41]. Maintaining high levels of DNA methylation is essential for promoting oocyte development [42]. In summary, these common differential metabolites suggest that the homogeneity of physiological and pathological ovarian aging may be related to oxidative stress, immune disorders, and inflammation.

The onset of ovarian aging is insidious, and the diagnostic criteria in the early stages are not sufficiently specific. Therefore, it is difficult to diagnose it physiologically or pathologically in the early stages. Testosterone sulfate, one of the specific differential metabolites of physiological ovarian aging, showed high diagnostic efficacy and accuracy, with an AUC of 0.929 and a Youden's index of 0.84. Testosterone sulfate is the main metabolite of testosterone, and decreased testosterone levels are associated with poor ovarian function [43]. Additionally, testosterone sulfate was negatively correlated with menaquinone and neopterin levels. Currently, there are no specific biomarkers for diagnosing physiological ovarian aging, apart from age itself. Our findings suggest that testosterone sulfate could serve as a potential diagnostic marker for early-stage physiological ovarian aging, offering clinicians a more precise tool for early detection and intervention.

The DOR, scPOI, and POI represent different stages of pathological ovarian aging. DOR and scPOI overlap in diagnostic criteria. Although the DOR patients selected in this study showed different bFSH levels than scPOI patients, these two groups shared three common differential lipid metabolites. All showed significantly decreased PC (18:2e/17:2), PC (17:0/18:2) and SM (d22:1/14:1) levels. PC, classified as a glycerophospholipid, is another lipid found in common differential metabolites. Previous studies [44, 45] showed that PC could promote inflammatory cytokine expression and polarizes macrophage activation toward the M1 phenotype. In recent years, more and more studies [46, 47] have shown that chronic inflammatory aging is closely related to decreased ovarian function. The DOR and scPOI groups showed significant differences compared to the POI group. SM (14:1/20:1) and 4-hydroxyretinoic acid levels significantly decreased in both the DOR and POI groups. Additionally, 4-hydroxyretinoic acid demonstrated high diagnostic efficacy in diagnosing POI, with an AUC of 0.921 and a Youden's index of 0.789. These values exceed those reported for previously studied plasma markers, which typically show AUCs ranging from 0.804 to 0.901 [22]. This highlights the superior diagnostic potential of 4-hydroxyretinoic acid in distinguishing POI from other forms of ovarian aging, further enhancing the accuracy of clinical assessments. 4-Hydroxyretinoic acid is an NADPH-dependent hydroxylated metabolite of retinoic acid. Retinoic acid, a derivative of vitamin A, plays an important role in germ cell development. Retinoic acid is critical for initiating meiosis in germ cells of fetal ovaries [48]. It could also promote folliculogenesis directly or through regulating gonadotropin-releasing hormone (GnRH) production and release [49, 50]. Additionally, it can regulate ovarian steroidogenesis by influencing the expression or activity of steroidogenic enzymes, such as steroidogenic acute regulatory protein (STAR), cytochrome P450 family 17 subfamily A member 1 (CYP17A1), and cytochrome P450 family 11 subfamily A member 1 (CYP11A1) [51]. These common differential metabolites represented the homogeneity of pathological ovarian aging.

Differences were also observed between pathological ovarian aging groups. 9-[(2-hydroxyethoxy)methyl]-1,9-dihydro-6 H-purin-6-one and taurocholic acid were representative metabolites in the DOR group. Taurocholic acid is classified to conjugated bile acid and could effectively relieve aging. Cassandra et al. found that taurocholic acid could protect against both degenerative and neovascular age-related macular degeneration through inhibiting vascular endothelial growth factor (VEGF)-induced choroidal endothelial cell migration and tube formation [52]. Tauroursodeoxycholic acid, derivative metabolites of taurocholic acid, could relieve ovarian

aging through rebuilding the damaged endoplasmic reticulum in ovarian surface epithelium [53].

Upregulated cholesteryl sulfate and downregulated choline were representative metabolites in the scPOI group. Cholesteryl sulfate is one of the most important known sterol sulfates in human plasma. It serves as not only a part of many biological membranes but also a substrate for the synthesis of sulfonated adrenal steroids such as pregnenolone. In vitro study showed that cholesteryl sulfate could modulate brain energy and its neuroprotective effects may be related to activating AKT signaling [54]. Another study found that cholesteryl sulfate levels in women's hair would decrease with age [55], which is different from the pathological ovarian aging. Excessive levels can also inhibit ovarian steroidogenesis by regulating the expression of mitochondrial P450 side chain cleavage (P450scc) and STAR [56]. Additionally, a targeted metabolomics study showed that polyunsaturated choline plasmalogens in the follicle fluid were significantly downregulated in women with DOR [57].

Vitamin A was specifically downregulated in the POI group. Vitamin A, also named retinol, is the precursor of retinoic acid. Retinol metabolism has received considerable attention in the context of ovarian aging. In addition to promoting the meiosis of germ cells, folliculogenesis, and steroidogenesis, retinoic acid can also stimulate the differentiation of oogonial stem cells and oogenesis [58]. The importance of retinol metabolism in egg regeneration inspired us to investigate treatments for ovarian aging. Additionally, the metabolic pathways involved in vitamin digestion and absorption and retinol metabolism were significant. It has been reported that vitamins C and E have anti-oxidative stress effects and can relieve mitochondrial function, which could restore the follicle reserve in ovarian aging mice [59, 60].

Conclusion

This study identified that both physiological and pathological ovarian aging share metabolic similarities involving disruptions in lipid, folate, and ubiquinone pathways. However, distinct differences were observed, with physiological and pathological aging displaying unique alterations in lipid, vitamin, and retinol metabolism. These findings not only contribute to better diagnostic capabilities but also open avenues for therapeutic advancements, as early identification of ovarian aging can inform personalized treatment strategies aimed at preserving ovarian function.

Limitation

Although untargeted metabolomics enables the detection of a broader spectrum of metabolites compared to targeted metabolomics, its accuracy may be compromised due to the inherent complexity of the technique. Serum

markers, while useful for systemic metabolomic profiling, may not fully capture ovarian-specific metabolic changes, as they can be influenced by broader systemic factors. Follicular fluid, in contrast, offers a potentially more accurate reflection of ovarian metabolism. However, obtaining follicular fluid in the early stages of ovarian aging presents significant challenges, making serum analysis a more practical alternative for this study. Additionally, the relatively small sample size of this study may limit the statistical power and generalizability of the findings. Given the progressive and potentially systemic nature of ovarian aging, larger, long-term studies are necessary to enhance the robustness of diagnostic capabilities and to better understand the broader impacts and complications associated with ovarian aging.

Abbreviations

AA	Arachidonic acid
AMH	Anti-Müllerian hormone
ANOVA	One-way analysis of variance
AUC	Area under the curve
BCAAs	Ranched chained amino acids
bE2	Basic estradiol
bFSH	basic follicle-stimulating hormone
bLH	basic luteinizing hormone
BMI	Body mass index
bT	basic testosterone
Ctrl	Control
CX3CR1	C-X-C Motif Chemokine Receptor 3
CYP11A1	Cytochrome P450 family 11 subfamily A member 1
CYP17A1	Cytochrome P450 family 17 subfamily A member 1
DOR	Diminished ovarian reserve
FC	Fold change
GnRH	Gonadotropin-releasing hormone
GTP	Guanosine-5'-triphosphate
HETE	Hydroxyeicosatetraenoic acid
HMDB	The Human Metabolome Database
KEGG	The Kyoto Encyclopedia of Genes and Genomes
NLRP3	Nucleotide-binding oligomerization domain-like receptor protein 3
OPLS-DA	Orthogonal projections to latent structure discriminant analysis
PC	Phosphoglyceride
PCA	Principal component analysis
PG	Phosphoglyceride
POI	Premature ovarian insufficiency
POR	Poor ovarian response
QC	Quality control
scPOI	subclinical premature ovarian insufficiency
SD	Standard deviation
SM	Sphingomyelin
STAR	Steroidogenic acute regulatory protein
VEGF	Vascular endothelial growth factor
VIP	Variable importance in the projection

Supplementary Information

The online version contains supplementary material available at <https://doi.org/10.1186/s13048-025-01625-2>.

Supplementary Material 1
Supplementary Material 2
Supplementary Material 3
Supplementary Material 4
Supplementary Material 5

Supplementary Material 6

Supplementary Material 7

Acknowledgements

We thank all the patients and volunteers participated in the study, and we also thank Lingnan Medical Research Center of Guangzhou University of Chinese Medicine, the Gynecology Laboratory of Guangzhou University of Chinese Medicine for providing relevant facilities.

Author contributions

Lihua Zeng, Ling Zhu and Songping Luo designed the study. Lihua Zeng, Yunyi Liang and Ling Zhu wrote the main manuscript, prepared all the figures. Lihua Zeng, Yunyi Liang and Lizhi Huang did the experiments. Lihua Zeng and Zu'ang Li analyzed the data. Manish Kumar, Xiasheng Zheng and Jing Li revised the manuscript. All authors read and approved the final manuscript.

Funding

This work was supported by National Natural Science Foundation of China (No.82174418) and Postdoctoral Fellowship Program (Grade C) of China Postdoctoral Science Foundation (No.GZC20232689).

Data availability

Data is available at www.ebi.ac.uk/metabolights/MTBLS10001 and www.ebi.ac.uk/metabolights/MTBLS10028.

Declarations

Consent for publication

Not applicable.

Competing interests

The authors declare no competing interests.

Human ethics and consent to participate

This study was approved by the Ethics Committee of First Affiliated Hospital of Guangzhou University of Chinese Medicine (No. JY2022-002). Informed consent was obtained from all the participants prior to sample collection.

Author details

¹Department of Gynecology, First Affiliated Hospital, Guangzhou University of Chinese Medicine, Guangzhou 510405, China

²Lingnan Medical Research Center of Guangzhou, University of Chinese Medicine, Guangzhou 514056, China

³Guangzhou University of Chinese Medicine, Guangzhou 510405, China

⁴CAS Key Laboratory of Regenerative Biology, South China Institute for Stem Cell Biology and Regenerative Medicine, Guangzhou Institutes of Biomedicine and Health, Chinese Academy of Sciences, Guangzhou, China

Received: 26 November 2024 / Accepted: 13 February 2025

Published online: 17 March 2025

References

1. Younis JS. Ovarian aging and implications for fertility female health. *Minerva Endocrinol (Torino)*. 2012;37(1):41–57.
2. Yang Q, Chen W, Cong L, Wang M, Li H, Wang H, et al. Nadase cd38 is a key determinant of ovarian aging. *Nat Aging*. 2024;4(1):110–28.
3. Cavalcante MB, Sampaio O, Camara F, Schneider A, de Avila BM, Prosczek J, et al. Ovarian aging in humans: potential strategies for extending reproductive lifespan. *Geroscience*. 2023;45(4):2121–33.
4. Park SU, Walsh L, Berkowitz KM. Mechanisms of ovarian aging. *Reproduction*. 2021;162(2):R19–33.
5. Laisk T, Tsuiko O, Jatsenko T, Horak P, Ojala M, Lahdenpera M, et al. Demographic and evolutionary trends in ovarian function and aging. *Hum Reprod Update*. 2019;25(1):34–50.

6. Li J, Xiong M, Fu XH, Fan Y, Dong C, Sun X, et al. Determining a multimodal aging clock in a cohort of Chinese women. *Med (NY)*. 2023;4(11):825–e84813.
7. Webber L, Davies M, Anderson R, Bartlett J, Braat D, Cartwright B, et al. Eshre guideline: management of women with premature ovarian insufficiency. *Hum Reprod*. 2016;31(5):926–37.
8. Ding T, Yan W, Zhou T, Shen W, Wang T, Li M, et al. Endocrine disrupting chemicals impact on ovarian aging: evidence from epidemiological and experimental evidence. *Environ Pollut*. 2022;305:119269.
9. Ruth KS, Day FR, Hussain J, Martinez-Marchal A, Aiken CE, Azad A, et al. Genetic insights into biological mechanisms governing human ovarian ageing. *Nature*. 2021;596(7872):393–7.
10. Stentz NC, Griffith KA, Perkins E, Jones RD, Jagsi R. Fertility and childbearing among American female physicians. *J Womens Health (Larchmt)*. 2016;25(10):1059–65.
11. Devine K, Mumford SL, Wu M, Decherney AH, Hill MJ, Propst A. (2015) Diminished ovarian reserve in the united States assisted reproductive technology population: diagnostic trends among 181,536 cycles from the society for assisted reproductive technology clinic outcomes reporting system. *Fertil Steril*. 104(3), 612–19.e3.
12. Polyzos NP, Blockeel C, Verpoest W, De Vos M, Stoop D, Vloeberghs V, et al. Live birth rates following natural cycle Ivf in women with poor ovarian response according to the Bologna criteria. *Hum Reprod*. 2012;27(12):3481–6.
13. Chon SJ, Umair Z, Yoon MS. Premature ovarian insufficiency: past, present, and future. *Front Cell Dev Biol*. 2021;9:672890.
14. Li M, Zhu Y, Wei J, Chen L, Chen S, Lai D. The global prevalence of premature ovarian insufficiency: a systematic review and meta-analysis. *Climacteric*. 2023;26(2):95–102.
15. Zhang A, Sun H, Wang X. Serum metabolomics as a novel diagnostic approach for disease: a systematic review. *Anal Bioanal Chem*. 2012;404(4):1239–45.
16. Qiu S, Cai Y, Yao H, Lin C, Xie Y, Tang S, Zhang A. Small molecule metabolites: discovery of biomarkers and therapeutic targets. *Signal Transduct Target Ther*. 2023;8(1):132.
17. Xue Z, Chen X, Li J. Metabolic disorder: the dark side of ovarian aging. *Trends Mol Med*. 2024;30(8):705–7.
18. Auro K, Joensuu A, Fischer K, Kettunen J, Salo P, Mattsson H, et al. A metabolic view on menopause and ageing. *Nat Commun*. 2014;5:4708.
19. Ding S, Chen M, Liao Y, Chen Q, Lin X, Chen S, et al. Serum metabolic profiles of Chinese women with perimenopausal obesity explored by the untargeted metabolomics approach. *Front Endocrinol (Lausanne)*. 2021;12:637317.
20. Liang C, Zhang X, Qi C, Hu H, Zhang Q, Zhu X, Fu Y. UHPLC-MS/MS analysis of Oxylipins metabolomics components of follicular fluid in infertile individuals with diminished ovarian reserve. *Reprod Biol Endocrinol*. 2021;19(1):143.
21. Khajeh M, Rahbarghazi R, Nouri M, Darabi M. Potential role of polyunsaturated fatty acids, with particular regard to the signaling pathways of arachidonic acid and its derivatives in the process of maturation of the oocytes: contemporary review. *Biomed Pharmacother*. 2017;94:458–67.
22. Zhou XY, Li X, Zhang J, Li Y, Wu XM, Yang YZ, et al. Plasma metabolomic characterization of premature ovarian insufficiency. *J Ovarian Res*. 2023;16(1):2.
23. Song H, Qin Q, Yuan C, Li H, Zhang F, Fan L. Metabolomic profiling of poor ovarian response identifies potential predictive biomarkers. *Front Endocrinol (Lausanne)*. 2021;12:774667.
24. Moslehi N, Mirmiran P, Marzbani R, Rezadoost H, Mirzaie M, Azizi F, et al. Serum metabolomics study of women with different annual decline rates of anti-mullerian hormone: an untargeted gas chromatography-mass spectrometry-based study. *Hum Reprod*. 2021;36(3):721–33.
25. Chen ZJ, Tian QJ, Qiao J. Chinese expert consensus on premature ovarian insufficiency. *Zhonghua Fu Chan Ke Za Zhi*. 2017;52(9):577–81.
26. Tal R, Seifer DB. Ovarian reserve testing: a user's guide. *Am J Obstet Gynecol*. 2017;217(2):129–40.
27. Campisi J, Kapahi P, Lithgow GJ, Melov S, Newman JC, Verdin E. From discoveries in ageing research to therapeutics for healthy ageing. *Nature*. 2019;571(7764):183–92.
28. Carrer DC, Schreier S, Patrito M, Maggio B. Effects of a short-chain ceramide on bilayer domain formation, thickness, and chain mobility: Dmpc and asymmetric ceramide mixtures. *Biophys J*. 2006;90(7):2394–403.
29. Dupuy FG, Maggio B. N-acyl chain in ceramide and sphingomyelin determines their mixing behavior, phase State, and surface topography in Langmuir films. *J Phys Chem B*. 2014;118(27):7475–87.
30. Cutler RG, Mattson MP. Sphingomyelin and ceramide as regulators of development and lifespan. *Mech Ageing Dev*. 2001;122(9):895–908.
31. Mohammadzadeh HN, Zarezadeh M, Molsberry SA, Ascherio A. Changes in plasma phospholipids and sphingomyelins with aging in men and women: a comprehensive systematic review of longitudinal cohort studies. *Ageing Res Rev*. 2021;68:101340.
32. Welsh J, Bak MJ, Narvaez CJ. New insights into vitamin K biology with relevance to cancer. *Trends Mol Med*. 2022;28(10):864–81.
33. Elkattawy HA, Ghoneim FM, Eladl MA, Said E, Ebrahim HA, El-Shafey M et al. (2022) Vitamin k2 (menaquinone-7) reverses age-related structural and cognitive deterioration in naturally aging rats. *Antioxid (Basel)*. 11(3).
34. Ma ML, Ma ZJ, He YL, Sun H, Yang B, Ruan BJ, et al. Efficacy of vitamin k2 in the prevention and treatment of postmenopausal osteoporosis: a systematic review and meta-analysis of randomized controlled trials. *Front Public Health*. 2022;10:979649.
35. Spencer ME, Jain A, Matteini A, Beamer BA, Wang NY, Leng SX, et al. Serum levels of the immune activation marker neopterin change with age and gender and are modified by race, Bmi, and percentage of body fat. *J Gerontol Biol Sci Med Sci*. 2010;65(8):858–65.
36. Hearps AC, Martin GE, Angelovich TA, Cheng WJ, Maisa A, Landay AL, et al. Aging is associated with chronic innate immune activation and dysregulation of monocyte phenotype and function. *Aging Cell*. 2012;11(5):867–75.
37. Jackaman C, Radley-Crabb HG, Soffe Z, Shavlakadze T, Grounds MD, Nelson DJ. Targeting macrophages rescues age-related immune deficiencies in c57bl/6j geriatric mice. *Aging Cell*. 2013;12(3):345–57.
38. Tiemeier H, Fekkes D, Hofman A, van Tuijl HR, Kiliaan AJ, Breteler MM. Plasma pterins and folate in late life depression: the Rotterdam study. *Psychiatry Res*. 2006;145(2–3):199–206.
39. Strandgaard T, Foder S, Heuck A, Ernst E, Nielsen MS, Lykke-Hartmann K. Maternally contributed folate receptor 1 is expressed in ovarian follicles and contributes to preimplantation development. *Front Cell Dev Biology*. 2017;5:89.
40. Liu T, Liu Y, Huang Y, Chen J, Yu Z, Chen C, et al. miR-15b induces premature ovarian failure in mice via inhibition of α -klotho expression in ovarian granulosa cells. *Free Radic Biol Med*. 2019;141:383–92.
41. Crott JW, Liu Z, Keyes MK, Choi SW, Jang H, Moyer MP, et al. Moderate folate depletion modulates the expression of selected genes involved in cell cycle, intracellular signaling and folate uptake in human colonic epithelial cell lines. *J Nutr Biochem*. 2008;19(5):328–35.
42. Yan R, Gu C, You D, Huang Z, Qian J, Yang Q, et al. (2021) Decoding dynamic epigenetic landscapes in human oocytes using single-cell multi-omics sequencing. *Cell stem cell*. 28(9), 1641–1656.e7.
43. Antonio L, Pauwels S, Laurent MR, Vanschoubroeck D, Jans I, Billen J et al. (2018) Free testosterone reflects metabolic as well as ovarian disturbances in subfertile oligomenorrheic women. *Int J Endocrinol*. 2018, 7956951.
44. Qin X, Qiu C, Zhao L. Lysophosphatidylcholine perpetuates macrophage polarization toward classically activated phenotype in inflammation. *Cell Immunol*. 2014;289(1–2):185–90.
45. Chang MC, Lee JJ, Chen YJ, Lin SJ, Lin LD, Jain-Wen LE, et al. Lysophosphatidylcholine induces cytotoxicity/apoptosis and il-8 production of human endothelial cells: related mechanisms. *Oncotarget*. 2017;8(63):106177–89.
46. Said RS, El-Demerdash E, Nada AS, Kamal MM. Resveratrol inhibits inflammatory signaling implicated in ionizing radiation-induced premature ovarian failure through antagonistic crosstalk between silencing information regulator 1 (sirt1) and poly(adp-ribose) polymerase 1 (parp-1). *Biochem Pharmacol*. 2016;103:140–50.
47. Lliberos C, Liew SH, Zareie P, La Gruta NL, Mansell A, Hutt K. Evaluation of inflammation and follicle depletion during ovarian ageing in mice. *Sci Rep*. 2021;11(1):278.
48. Agrimons KS, Hogarth CA. Germ cell commitment to oogenic versus spermatogenic pathway: the role of retinoic acid. *Results Probl Cell Differ*. 2016;58:135–66.
49. Kanasaki H, Mijiddorj T, Sukhbaatar U, Oride A, Ishihara T, Yamagami I, et al. Trichostatin A reduces GnRH mRNA expression with a concomitant increase in retinaldehyde dehydrogenase in GnRH-producing neurons. *Mol Cell Endocrinol*. 2015;413:113–9.
50. Fujihara M, Yamamizu K, Comizzoli P, Wildt DE, Songsasen N. (2018) Retinoic acid promotes in vitro follicle activation in the Cat ovary by regulating expression of matrix metalloproteinase 9. *PLoS ONE*. 13(8), e0202759.
51. Dias NB, de Souza BM, Gomes PC, Brigatte P, Palma MS. Peptidome profiling of venom from the social Wasp polybia paulista. *Toxicon*. 2015;107:290–303.
52. Warden C, Barnett JM, Brantley MA Jr. Taurocholic acid inhibits features of age-related macular degeneration in vitro. *Exp Eye Res*. 2020;193:107974.

53. Vašíčková K, Moráň L, Gurín D, Vaňhara P. Alleviation of Endoplasmic reticulum stress by Tauroursodeoxycholic acid delays senescence of mouse ovarian surface epithelium. *Cell Tissue Res.* 2018;374(3):643–52.
54. Prah J, Winters A, Chaudhari K, Hersh J, Liu R, Yang SH. Cholesterol sulfate alters astrocyte metabolism and provides protection against oxidative stress. *Brain Res.* 2019;1723:146378.
55. Brosche T, Dressler S, Platt D. Age-associated changes in integral cholesterol and cholesterol sulfate concentrations in human scalp hair and finger nail clippings. *Aging (Milano).* 2001;13(2):131–8.
56. Tsutsumi R, Hiroi H, Momoeda M, Hosokawa Y, Nakazawa F, Koizumi M, et al. Inhibitory effects of cholesterol sulfate on progesterone production in human granulosa-like tumor cell line. *KGN Endocr J.* 2008;55(3):575–81.
57. de la Barca JMC, Boueilh T, Simard G, Boucret L, Ferré-L'Hotellier V, Tessier L, et al. Targeted metabolomics reveals reduced levels of polyunsaturated choline plasmalogens and a smaller dimethylarginine/arginine ratio in the follicular fluid of patients with a diminished ovarian reserve. *Hum Reprod.* 2017;32(11):2269–78.
58. Zou K, Wang J, Bi H, Zhang Y, Tian X, Tian N et al. (2019) Comparison of different in vitro differentiation conditions for murine female germline stem cells. *Cell Prolif.* 52(1), e12530.
59. Abdollahifar MA, Azad N, Sajadi E, Shams MZ, Zare F, Moradi A, et al. Vitamin C restores ovarian follicular reservation in a mouse model of aging. *Anat Cell Biol.* 2019;52(2):196–203.
60. Omidi M, Ahangarpour A, Ali MS, Khorsandi L. The effects of myricitrin and vitamin e against reproductive changes induced by d-galactose as an aging model in female mice: an experimental study. *Int J Reprod Biomed.* 2019;17(11):789–98.

Publisher's note

Springer Nature remains neutral with regard to jurisdictional claims in published maps and institutional affiliations.